Chirality Transfer from Guest Chiral Metal Complexes to Inorganic Framework: The Role of Hydrogen Bonding

Yu Wang, Jihong Yu,* Yi Li, Zhan Shi, and Ruren Xu*[a]

Abstract: The structure elucidation of a new zinc phosphate $[Co^{II}(en)_3][Zn_4(H_2PO_4)_3(HPO_4)_2(PO_4)(2H_2O)_2]$ (**1**) reveals that the racemic cobalt complex templates the zinc phosphate framework in such a way that the local C_2 point symmetry of the structural motif of the inorganic framework conforms with that of the cobalt complex pairing with it, in essence transferring its chirality to the inorganic host. An analysis of hydrogen bonding between the guest molecules and the inorganic host framework reveals that hydrogen bonding is responsible for the stereospecific structural arrangement. Upon examining previously reported chiral metal-complex-templated structures of metal phosphates, it is revealed that such hydrogen bonding is the common origin for inducing chirality transfer in metal–phosphate frameworks templated with chiral metal complexes. Crystal data of **1**: orthorhombic, *Pbcn* (no. 60), $a = 10.4787(8)$ Å, $b = 20.0091(14)$ Å, $c = 14.9594(10)$ Å, and $Z = 2$.

Keywords: chirality transfer · host–guest systems · hydrogen bonds · hydrothermal synthesis · structure elucidation

Introduction

Chiral molecular sieves attract considerable attention, because of their potential application in enantioselective catalysis and separations.[1] There have been three general methodologies that have been employed for obtaining chiral molecular sieves. One is to modify an existing inorganic material with a chiral organic component through either intercalation[2] or surface anchoring.[3, 4] The second is to incorporate chiral moieties into the building blocks of an organic–inorganic hybrid framework constructed through coordination of the organic component to metal cations.[5] The third approach is to impart chirality to an as-synthesized inorganic open-framework by using a chiral template. The first two approaches have been remarkably successful. For example, by using chirally modified zeolites as catalysts,[3, 4] stereoselective photoreactions have been achieved; therefore, racemic mixtures of small organic molecules have been resolved using materials obtained by the second approach.[5] However, the third approach to chiral molecular sieves, in spite of some remarkable effort, has led to few successes.[6] Optically pure chiral zeolitic material has never been made, even though it has long been recognized that both zeolite β[1, 7] and ETS-10[8] are heavily intergrown materials with one of the polymorphs being chiral.

Inasmuch as no chiral template is necessary for the formation of a chiral zeolitic polymorph, a small number of metal phosphates with a chiral framework have also been prepared by using achiral templates, such as $[Na_{12}(H_2O)_{12}][Zn_{12}P_{12}O_{48}]$,[9] $[NH_3(CH_2)2NH_2(CH_2)2NH_3][(ZnPO_4)HPO_4]$,[10] $[CN_3H_6][Sn_4P_3O_{12}]$,[11] $[CH_32NH_2]K_4[V_{10}O_{10}(H_2O)_2(OH)_4(PO_4)_7]\cdot 4H_2O$,[12] ULM-5,[13] UCSB-7,[14] and $[Ti_3P_6O_{27}]\cdot 5[NH_3CH_2CH_2NH_3]\cdot 2H_3O$.[15] Since no part of the initial reaction mixture is intrinsically chiral, their bulk products are invariably 50:50 mixtures of enantiomeric crystals.

The lack of success to impart chirality from a template to a molecular sieve is perhaps due to, firstly, a lack of understanding of the interactions between a template and a corresponding framework. Furthermore, it may not have been appreciated that, in order for transfer of chirality to occur, multipoint cooperative non-covalent interactions stronger than van der Waals forces are perhaps necessary. As a starting point for understanding the role of a chiral template in determining the stereospecificity of an inorganic framework structure, we have chosen metal phosphate systems that are known to incorporate chiral metal complexes and in which extensive hydrogen bonding between the template and the inorganic host is possible. We have chosen to focus on the role of hydrogen bonding, because it has been suggested to play a role in inducing chirality in an aluminophosphate with a chiral template,[16] and multiple hydrogen bonds are known to cooperatively exert dramatic influences

[a] Prof. J. Yu, Prof. R. Xu, Y. Wang, Y. Li, Dr. Z. Shi
State Key Laboratory of Inorganic Synthesis and Preparative Chemistry, College of Chemistry, Jilin University
Changchun 130023, (P.R. China)
Fax: (+86) 431-567-1974
E-mail: jihong@mail.jlu.edu.cn, rrxu@mail.jlu.edu.cn

DOI: 10.1002/chem.200305040

on the supramolecular assemblies in chemical and biological systems.[17]

Among the large number of open-framework metal phosphates,[18–20] several metal phosphates templated by chiral metal complexes have become known recently, including aluminophosphates,[16, 21–24] gallium phosphate [Δ-$Co(en)_3$]-[$H_3Ga_2P_4O_{16}$],[25] [$Co(en)_3$][$Ga_3(H_2PO_4)_6(HPO_4)_3$],[26] boron phosphate [$Co(en)_3$][$B_2P_3O_{11}(OH)_2$],[27] and zinc phosphates, [$Co^{II}(en)_3$]$_2$[$Zn_6P_8O_{32}H_8$], and [$Co^{III}(en)_3$][$Zn_8P_6O_{24}Cl$]·$2H_2O$.[28] More recently, by using a racemic mix of chiral [$Co(dien)_2$]Cl_3 complex as the template, an interesting open-framework zinc phosphate H_3O[$Co(dien)_2$][$Zn_2(HPO_4)_4$] has been prepared with multidirectional helical channels.[29] The rigid octahedrally coordinated metal amine complex is chiral, which exists as both the Δ and Λ enantiomers. As has been demonstrated in the recent work by Morgan[16] and by us,[28, 29] a chiral inorganic structural motif can be induced by the chiral complex template.

In this work, the synthesis of a new zinc phosphate by using a racemic mixture of the chiral metal complexes, [$Co(en)_3$]Cl_3, is reported. The single-crystal structure solution of this compound, and the analysis of the hydrogen bonding between the template and the host reveal that there exists a stereospecificity between the template and the host, and that hydrogen bonding is its origin. Further examination of this type of chiral molecular-recognition phenomenon in several previously reported metal phosphates templated by chiral complexes identifies, for the first time, a common chiral configuration and symmetry in their inorganic microenvironment as a result of chirality transfer from chiral metal complexes.

Experimental Section

Synthesis: The title compound was prepared by means of a hydrothermal reaction between $Zn(OAc)_2\cdot 2H_2O$, H_3PO_4, [$Co(en)_3$]Cl_3 and H_2O in a molar ratio of 1:3:0.5:488. Typically, $Zn(OAc)_2\cdot 2H_2O$ (0.25 g) was dissolved in H_2O (10 mL), and then H_3PO_4 (85 wt%, 0.23 mL) was added and stirred. Finally, [$Co(en)_3$]Cl_3 (0.22 g) was added to the above reaction mixture. The resulting gel was stirred for one hour until it was homogeneous, and it was then sealed in a Teflon-lined stainless steel autoclave and heated at 110 °C for 26 hours under static condition. The product, which contained orange plate-shaped single crystals, was separated by sonication, and further washed with distilled water and then air-dried. The X-ray diffraction pattern of the product was in good agreement with that generated from single-crystal structural data; this confirmed the phase purity of the as-synthesized product.

Characterization: X-ray powder diffraction (XRD) data were collected on a Siemens D5005 diffractometer with $Cu_{K\alpha}$ radiation ($\lambda = 1.5418$ Å).

Inductively coupled plasma (ICP) analysis was performed on a Perkin–Elmer Optima 3300DV spectrometer. The determined data (Zn, 23.5% wt P, 16.7% wt Co, 5.30% wt) are in agreement with those calculated values (Zn, 22.9% wt P, 16.1% wt Co, 5.27% wt). The elemental analysis was conducted on a Perkin–Elmer 2400 elemental analyzer. The determined data (C, 6.48% wt H, 3.15% wt N, 7.55% wt) are in agreement with those calculated values (C, 6.37% wt H, 3.90% wt N, 7.38% wt).

A Perkin–Elmer TGA 7 unit was used to carry out the thermogravimetric analysis (TGA) in air with a heating rate of 10 °C min^{-1}. A weight loss of 20% in total (calcd 21.5%), which occurred at 200–660 °C was observed; this was attributed to the dehydration of the product and the decomposition of the metal complex.

Structural determination: A suitable single crystal with dimensions of $0.20 \times 0.05 \times 0.04$ mm was selected for single-crystal X-ray diffraction analysis. Structural analysis was performed on a Siemens SMART CCD diffractometer by using graphite-monochromated $Mo_{K\alpha}$ radiation ($\lambda = 0.71073$ Å). The data were collected at temperature of 20 ± 2 °C.

Intensity data of 14343 reflections of which 2251 were independent ($-11 \ll h \ll 10$, $-22 \ll k \ll 19$, $-16 \ll l \ll 14$) were collected in the ω scan mode ($R_{int} = 0.0588$).

Data processing was accomplished with the SAINT processing program.[30] The structure was solved in the space group *Pbcn* by the direct methods, and was refined on F^2 by full-matrix least-squares by using SHELXTL97.[31] All Zn, Co, P, and O atoms were easily located. Hydrogen atoms that were attached to the terminal P–O groups and to the metal complex cation were placed geometrically, and were refined by using a riding model. Zn(2) was disordered over two sites.

All non-hydrogen atoms were refined anisotropically. Experimental details for the structure determination are presented in Table 1. The atomic coordinates, and the selected bond lengths and angles are presented in Tables 2 and 3, respectively. CCDC-208133 contains the supplementary crystallographic data for this paper. These data can be obtained free of charge via www.ccdc.cam.ac.uk/conts/retrieving.html (or from the Cambridge Crystallographic Data Centre, 12 Union Road, Cambridge CB2 1EZ, UK; fax: (+44) 1223-336-033; or e-mail: deposit@ccdc.cam.ac.uk).

Table 1. Crystal data and structure refinement for [$Co^{II}(en)_3$]-[$Zn_4(H_2PO_4)_3(HPO_4)_2(PO_4)(H_2O)_2$].

formula	$C_6H_{36}CoN_6O_{26}P_6Zn_4$
M_r	1112.64
T [K]	293(2)
λ [Å]	0.71073
crystal system, space group	orthorhombic, *Pbcn*
a [Å]	10.4787(8)
b [Å]	20.0091(14)
c [Å]	14.9594(10)
V [Å^3]	3136.5(4)
Z/ρ_{calcd} [Mg m^{-3}]	4/2.356
μ [mm^{-1}]	3.949
F(000)	2228
crystal size [mm]	$0.20 \times 0.05 \times 0.04$
θ range [°]	2.04–23.23
reflections collected/unique	14343/2251 [R(int) = 0.0588]
completeness to $\theta = 23.23$ [%]	99.7
absorption correction	empirical
transmission max/min	0.8580/0.5056
data/restraints/parameters	2251/0/232
goodness of fit	1.063
final R indices [$I > 2\sigma(I)$]	$R_1 = 0.0538$, $wR_2 = 0.1446$
R indices (all data)	$R_1 = 0.0689$, $wR_2 = 0.1532$
largest difference peak/hole [e Å^{-3}]	1.887/−1.047

Computer simulations: The calculation was based on the Burchart 1.01-Dreiding 2.21 force field that combines the Burchart force field,[32] which was used to treat the frameworks of zeolites, and Dreiding II force field,[33] which was used to treat the intra- and intermolecular interactions. Because the energy terms for Co species were not addressed in this force field, we divided them into bonding and nonbonding terms.

For the bonding terms, we used a UFF generator, since the Universal force field facilitated the optimization for the configuration of the metal complexes.

For the nonbonding terms, we used Lennard–Jones 6–12 potential function to express the van der Waals energy. Some parameters not given in the Dreiding force field were added according to the reference;[34] which were as follows: Co···O: $D_0 = 0.055$ kcal mol^{-1}, $R_0 = 3.18$ Å; Co···H: $D_0 = 0.055$ kcal mol^{-1}, $R_0 = 2.16$ Å. Other parameters were the same as those used in Burchart 1.01—Dreiding 2.21 force field given in the Cerius^2 package.[35] The hydrogen bonding energies between the host inorganic network and the guest template molecules were studied in this work. The

Table 2. Atomic coordinates [$\times 10^4$] and equivalent isotropic displacement parameters [$Å^2 \times 10^3$] for $[Co^{II}(en)_3][Zn_4(H_2PO_4)_3(HPO_4)_2(PO_4)(H_2O)_2]$ U(eq) is defined as one third of the trace of the orthogonalized U_{ij} tensor.

	x	y	z	U(eq)
Zn(1)	735(1)	2437(1)	8866(1)	32(1)
Zn(2)	4057(2)	889(1)	10658(1)	30(1)
Zn(2′)	3674(3)	839(1)	9821(2)	62(1)
Co(1)	0	1440(1)	12500	21(1)
P(1)	0	1198(2)	7500	40(1)
P(2)	0	3620(2)	7500	28(1)
P(3)	3077(2)	2343(1)	10215(1)	22(1)
P(4)	3636(3)	−587(1)	10790(2)	48(1)
O(1)	753(7)	1616(4)	8140(5)	60(2)
O(2)	800(6)	3209(4)	8112(5)	59(2)
O(3)	2450(5)	2542(3)	9348(3)	37(2)
O(4)	−542(5)	2420(3)	9796(4)	33(1)
O(5)	870(7)	689(3)	7019(5)	65(2)
O(6)	921(8)	4068(4)	6980(5)	72(2)
O(7)	2358(6)	2671(3)	11023(4)	35(1)
O(8)	2928(6)	1600(3)	10397(4)	43(2)
O(9)	3093(7)	63(3)	10505(5)	54(2)
O(10)	2559(8)	−1065(3)	11030(5)	64(2)
O(11)	4471(8)	−914(4)	10119(9)	110(4)
O(12)	4434(16)	−440(6)	11622(10)	194(8)
O(13)	2862(9)	818(4)	8634(6)	88(3)
N(1)	348(6)	1412(3)	11209(4)	30(2)
N(2)	1241(6)	2159(3)	12673(4)	28(2)
N(3)	1318(7)	766(3)	12753(5)	36(2)
C(1)	−252(10)	790(5)	10831(6)	43(2)
C(2)	564(8)	2806(4)	12802(5)	34(2)
C(3)	1545(9)	714(5)	13728(6)	45(2)

hypothetical structural models relevant to the experimental structures were built up by reversing the configuration of the complex cations followed by energy minimization. During energy minimization, the inorganic framework was fixed, and each Co complex cation was considered as a rigid body. The hypothetical structural model had the same space group as the experimental structure.

Results and Discussion

The structure of compound **1** consists of a macroanionic $[Co^{II}(en)_3][Zn_4(H_2PO_4)_3(HPO_4)_2(PO_4)(H_2O)_2]^{2-}$ framework. Charge neutrality is achieved by the metal complex cation $[Co(en)_3]^{2+}$. A cobalt cation has apparently been reduced during the hydrothermal synthesis process. While it is only speculated that labile ethylenediamine may be the reducing agent for the transformation of $[Co(en)_3]^{3+}$ to $[Co(en)_3]^{2+}$ during synthesis, it has been unambiguously established in a similar reaction system that the cobalt complex is indeed reduced under the hydrothermal synthesis conditions.[28] The asymmetric unit, as seen in Figure 1, contains two unique Zn atoms and four unique P atoms. Both Zn(1) and Zn(2) are tetrahedrally coordinated making four Zn-O-P linkages. Zn(2) is positionally disordered over two sites, with a lattice water molecule, O(13), that contributes to the coordination of Zn(2)′. The Zn–O distances are in the range of 1.890(6) to 1.979(8) Å. Three types of phosphate groups, $H_2PO_4^-$, HPO_4^{2-}, and PO_4^{3-}, are found to share their non-hydroxyl oxygen atoms with Zn atoms. The $P–O_{bridging}$ distances are in

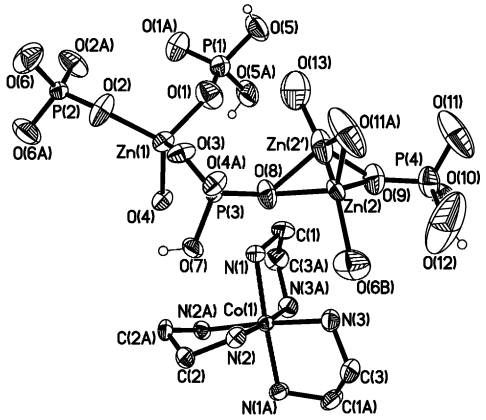

Figure 1. Thermal ellipsoid plot (50%) showing the labeling scheme in **1**.

the range of 1.482(7) to 1.530(7) Å. All the hydroxyl groups are free from bonding to Zn atoms, and have longer P–O distances in the range of 1.522(7) to 1.568(6) Å. Of the four distinct P atoms, P(1) and P(2) lie on a twofold axis, while P(3) and P(4) occupy general positions. As shown in Figure 1, each asymmetric unit also contains one unique Co atom lying on the twofold axis.

The Zn- and P-centered tetrahedra alternate to form a three-dimensional open framework with channels running along the [001] direction. A pair of enantiomeric $[Co(en)_3]^{2+}$ ions reside within the channel (Figure 2). Eight Zn and P

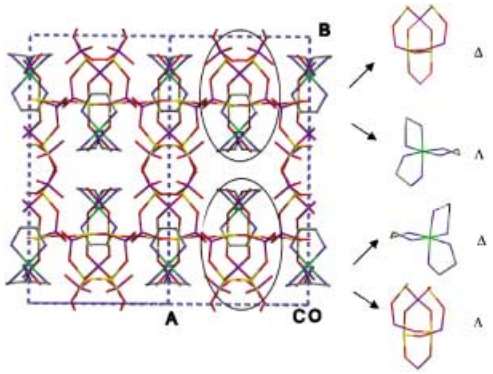

Figure 2. The open-framework structure of compound **1** viewed along the [001] direction (Zn(2′) atoms and water molecules are omitted for clarity). The chiral structural motif composed of three four-membered rings is associated with the chiral-metal complex cation with the same C_2 symmetry.

atoms form a 16-membered-ring window that circumscribes the channel opening. The channels are partially blocked by the $H_2PO_4^{2-}$ groups that protrude into the channel. It is helpful to view the inorganic framework as built from a simple structural motif composed of three four-membered rings. These structural motifs are stacked along the [001] direction and are linked together through bridging oxygen atoms, O(3) and O(4), along the [100] and [010] directions to form the three-dimensional open-framework. Notice that the motifs can twist in either the right- or left-handed direction along their symmetric axis. The former is denoted as Δ configuration and the latter as Λ configuration. The significance of describing the structure with such a structural motif becomes

Table 3. The selected bond lengths [Å] and angles [°] for $[Co^{II}(en)_3][Zn_4(H_2PO_4)_3(HPO_4)_2(PO_4)(H_2O)_2]$.[a]

Zn(1)−O(2)	1.913(6)	Zn(1)−O(4)	1.930(5)
Zn(1)−O(3)	1.948(5)	Zn(1)−O(1)	1.969(7)
Zn(2)−O(8)	1.890(6)	Zn(2)−O(11)#1	1.932(9)
Zn(2)−O(9)	1.952(7)	Zn(2)−O(6)#2	1.979(8)
Zn(2′)−O(8)	1.917(6)	Zn(2′)−O(11)#1	1.951(9)
Zn(2′)−O(9)	1.956(7)	Zn(2′)−O(13)	1.970(10)
P(1)−O(1)	1.496(7)	P(1)−O(1)#4	1.496(7)
P(1)−O(5)	1.544(7)	P(1)−O(5)#4	1.544(7)
P(2)−O(2)#4	1.489(6)	P(2)−O(2)	1.489(6)
P(2)−O(6)#4	1.530(7)	P(2)−O(6)	1.530(7)
P(3)−O(3)	1.507(6)	P(3)−O(8)	1.520(6)
P(3)−O(4)#5	1.523(6)	P(3)−O(7)	1.568(6)
P(4)−O(9)	1.482(7)	P(4)−O(11)	1.483(9)
P(4)−O(10)	1.522(7)	P(4)−O(12)	1.529(11)
O(2)-Zn(1)-O(4)	117.6(3)	O(2)-Zn(1)-O(3)	95.7(3)
O(4)-Zn(1)-O(3)	112.0(2)	O(2)-Zn(1)-O(1)	110.3(3)
O(4)-Zn(1)-O(1)	112.9(3)	O(3)-Zn(1)-O(1)	106.6(3)
O(8)-Zn(2)-O(11)#1	110.9(4)	O(8)-Zn(2)-O(9)	106.8(3)
O(11)#1-Zn(2)-O(9)	111.3(3)	O(8)-Zn(2)-O(6)#2	100.5(3)
O(11)#1-Zn(2)-O(6)#2126.2(5)	O(9)-Zn(2)-O(6)#2	99.2(3)	
O(8)-Zn(2′)-O(11)#1	108.9(3)	O(8)-Zn(2′)-O(9)	105.6(3)
O(11)#1-Zn(2′)-O(9)	110.3(4)	O(8)-Zn(2′)-O(13)	104.2(3)
O(11)#1-Zn(2′)-O(13)118.2(5)	O(9)-Zn(2′)-O(13)	108.7(3)	
O(1)-P(1)-O(1)#4	111.9(6)	O(1)-P(1)-O(5)	110.8(4)
O(1)#4-P(1)-O(5)	112.4(4)	O(1)-P(1)-O(5)#4	112.4(4)
O(1)#4-P(1)-O(5)#4	110.8(4)		
O(5)-P(1)-O(5)#4	97.6(5)		
O(2)#4-P(2)-O(2)	112.9(6)	O(2)#4-P(2)-O(6)#4	106.3(4)
O(2)-P(2)-O(6)#4	111.5(4)	O(2)#4-P(2)-O(6)	111.5(4)
O(2)-P(2)-O(6)	106.3(4)	O(6)#4-P(2)-O(6)	108.2(7)
O(3)-P(3)-O(8)	111.6(4)	O(3)-P(3)-O(4)#5	108.9(3)
O(8)-P(3)-O(4)#5	113.9(3)	O(3)-P(3)-O(7)	110.1(3)
O(8)-P(3)-O(7)	102.8(3)	O(4)#5-P(3)-O(7)	109.6(3)
O(9)-P(4)-O(11)	114.7(6)	O(9)-P(4)-O(10)	109.6(4)
O(11)-P(4)-O(10)	108.7(4)	O(9)-P(4)-O(12)	105.9(6)
O(11)-P(4)-O(12)	108.2(9)	O(10)-P(4)-O(12)	109.5(7)
P(1)-O(1)-Zn(1)	144.6(5)	P(2)-O(2)-Zn(1)	142.0(4)
P(3)-O(3)-Zn(1)	133.8(3)	P(3)#6-O(4)-Zn(1)	130.2(3)
P(1)-O(5)-H(5)	109.5	P(2)-O(6)-Zn(2)#7	122.7(5)
P(3)-O(7)-H(7)	109.5	P(3)-O(8)-Zn(2)	135.1(4)
P(3)-O(8)-Zn(2′)	130.9(4)	P(4)-O(9)-Zn(2)	120.8(4)
P(4)-O(9)-Zn(2′)	136.7(5)	P(4)-O(11)-Zn(2)#1	150.1(6)
P(4)-O(11)-Zn(2′)#1	121.5(7)	P(4)-O(12)-H(12)	109.5
P(4)-O(10)-H(10)	109.5		
D−H···A	d(D··A)	∢(DHA)	
O(5)-H(5)··O(10)#8	2.426(10)	162.5	
O(7)-H(7)··O(10)#9	2.531(8)	172.0	
O(12)-H(12)··O(12)#10	2.88(2)	108.4	
N(1)-H(1A)··O(4)	3.066(8)	155.9	
N(1)-H(1B)··O(8)	2.987(9)	156.3	
N(2)-H(2A)·vO(3)#2	2.919(8)	145.9	
N(2)-H(2B)··O(7)	2.917(8)	150.9	

[a] Symmetry transformations used to generate equivalent atoms: #1; $-x+1,-y,-z+2$ #2; $-x+1/2,-y+1/2,z+1/2$ #3; $-x,y,-z+5/2$ #4; $-x,y,-z+3/2$ #5; $x+1/2,-y+1/2,-z+2$ #6; $x-1/2,-y+1/2,-z+2$ #7; $-x+1/2,-y+1/2,z-1/2$ #8; $x,-y,z-1/2$; #9; $-x+1/2,y+1/2,z$; #10; $-x+1,y,-z+5/2$

apparent once it is recognized that the structural motif has the same C_2 symmetry as the chiral complex cation, and that each chiral structural motif is associated with a chiral metal-complex cation in such a way that the metal complex with the Δ configuration is in close contact with the chiral motif with the Λ configuration, and the metal complex with the Λ configuration is in close contact with the chiral motif that has the Δ configuration. This remarkable stereospecific correspondence between the metal-complex template and the structure of the inorganic host clearly indicates that molecular recognition between the guest and the host exists; this allows the configuration and symmetry information of the guest template to be passed onto the inorganic framework.

To understand the cause for the observed chiral molecular recognition, a detailed hydrogen-bonding network that involves the metal complex and the inorganic structure has been analyzed. Figure 3 shows the hydrogen-bonding arrangement between the complex cations and the nearby chiral structural motifs in **1**. The hydrogen bonds are all of N−H···O type, and the N···O distances involved in the hydrogen bonding are in the range of 2.917–3.066(8) Å. These hydrogen bond distances are within the range expected for this type of bonding.[36] Each $[Co(en)_3]^{2+}$ forms ten hydrogen bonds with four chiral inorganic structural motifs of the inorganic host nearby; these all have the same chirality. Namely the chiral structural motifs that have Λ configuration form hydrogen bonds with chiral complex cations that have Δ configuration, whilst the chiral structural motifs that have Δ configuration form hydrogen bonds with chiral complex cations with Λ configuration, as can be seen in Figure 3. This implies a chirally selective recognition, that is, a chiral discrimination effect. Having examined the hydrogen-bonding network, it is readily recognized that if a metal complex with the Λ configuration is to be inserted into the lattice position of the metal complex with the Δ configuration, or vice versa, the number of hydrogen bonds per cobalt complex will be reduced to eight in the reversed framework. The difference between the experimental structure and the reversed hypothetical structure of the hydrogen bond energy of the host–guest is $-27.13\ kJ\,mol^{-1}$ per complex.

As a consequence, the complex cations and the chiral structural motifs are related by a twofold axis. Therefore, the hydrogen bonding imposes the C_2 symmetry operation of the chiral complex template onto the chiral structural motif. This demonstrates that chiral molecular recognition between the guest and host occurs through hydrogen bonds.

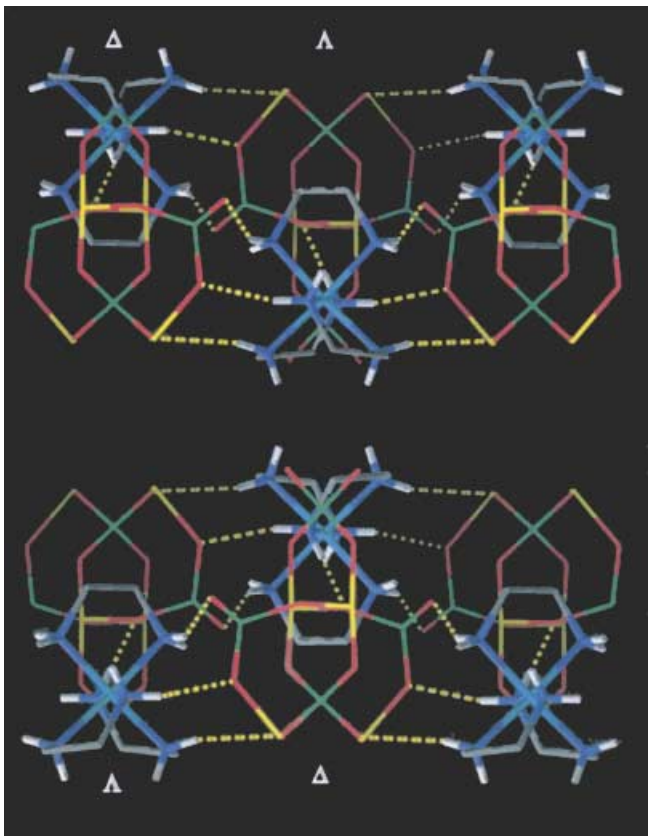

Figure 3. The hyrogen bonds between the complex templates and nearby chiral structural motifs in **1**.

The chiral aluminophosphate $[\Delta\text{-Co(en)}_3][Al_3P_4O_{16}]\cdot 3H_2O$ (**2**) is templated by an optically pure Δ-$[Co(en)_3]^{3+}$ cation.[21] It has a 2D-layered structure with 4.6-net, and is characteristic of a [3.3.3]propellane-like chiral structural motif (Figure 4).

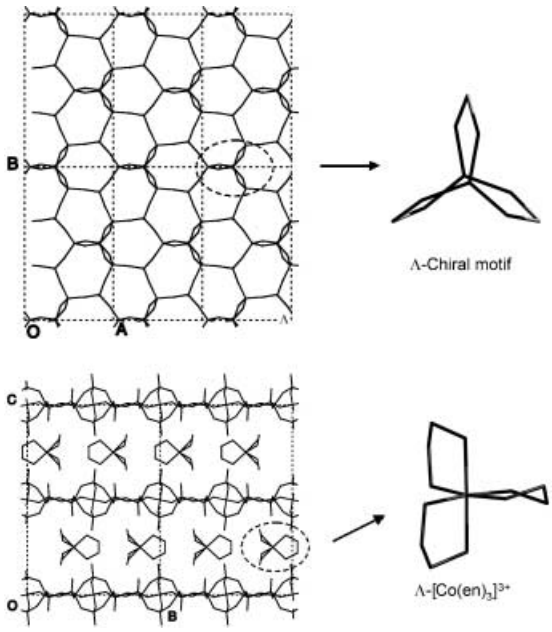

Figure 4. The 4.6-net sheet in **2**. The [3.3.3]propellane-like chiral motif and the chiral-metal complex occluded in the interlayer region are shown.

By extending our understanding of compound **1**, taking into account previously reported metal phosphates that are templated with either an optically pure or a racemic mixture of chiral metal complex, we find that the observed chirality transfer between the chiral templates and the inorganic host framework occurs by the symmetry correspondence between the chiral metal complex and the chiral structural motif. This template–host symmetry relationship in six-metal-complex-templated metal phosphates, including compound **1**, is shown in Table 4.

The chiral structural motif and the complex cation both have the same C_2 symmetry. Notably, the complex templates occluded in the interlayer region have the Λ configuration, and the chiral inorganic structural motifs exclusively have the Λ configuration. The stereospecific correspondence between the metal-complex template and the inorganic structural motifs can be well understood due to the fact that the number of hydrogen bonds will be reduced, and the hydrogen bond energy of the host–guest will be increased upon replacing the

Table 4. The template–host symmetry and configuration relationship in metal-complex-templated metal phosphates.

	Formula	Inorganic motif	Metal complex	Hydrogen bond interaction per Co complex		
				H-bond number in experimental structure[a]	H-bond number in hypothetical structure[a]	$\Delta E_{exp\text{-}hypo}$ [kJ mol^{-1}]
1	$[Co^{II}(en)_3][Zn_4(H_2PO_4)_3(HPO_4)_2(PO_4)(H_2O)_2]$	a pair of enatiomers of structural motif composed of three four-MRs (Δ and $\Lambda/C2$)	$[Co(en)_3]^{2+}$ (Δ and Λ/C_2)	10	8	– 27.13
2	$[\Delta\text{-Co(en)}_3][Al_3P_4O_{16}]\cdot 3H_2O$	[3.3.3]propellane-like motif ($\Lambda/C2$)	$[\Delta\text{-Co(en)}_3]^{3+}$ (Λ/C_2)	10	8	– 42.34
3	*trans*-$[Co(dien)_2][Al_3P_4O_{16}]\cdot 3H_2O$	[3.3.3]propellane-like motif ($\Lambda/C2$)	one enantiomer of $[Co(dien)_2]^{3+}$ (ion Λ/C_2)	4	0	– 44.85
4	$[Co(tn)_3][Al_3P_4O_{16}]\cdot 2H_2O$	capped 6-MR (Δ/C_1)	$Co(tn)_3$ (Δ/C_1)	9	7	– 15.05
5	$[Co^{II}(en)_3]_2[Zn_6P_8O_{32}H_8]$	[3.3.3]propellane-like motif (Δ and Λ/C_1)	$[Co(en)_3]^{2+}$ (Δ and $\Lambda/C_2$and C_1)	10	8	– 51.58
6	$[Co(en)_3][Zn_8P_6O_{24}Cl]\cdot 2H_2O$	caplike motif composed of six 4-MRs and three 3-MRs (Δ and Λ/C_3)	$[Co(en)_3]^{2+}$ (Δ and Λ/D_3)	12	6	– 79.88

[a] Only strong hydrogen bonds are considered ($H\cdots A < 2.5$ Å, $D{-}H\cdots A > 130^\circ$)

metal complex with the Λ configuration by its enantiomer in the framework (Table 4).

Compound **3**, a chiral layered aluminophosphate [*trans*-$Co(dien)_2][Al_3P_4O_{16}]\cdot 3H_2O$, contains chiral layers stacked in a helical fashion with only one enantiomer of the $[Co(dien)_2]^{3+}$ ions located in the interlayer region (Figure 5).[22] As with compound **2**, its 4.6-net sheet is featured

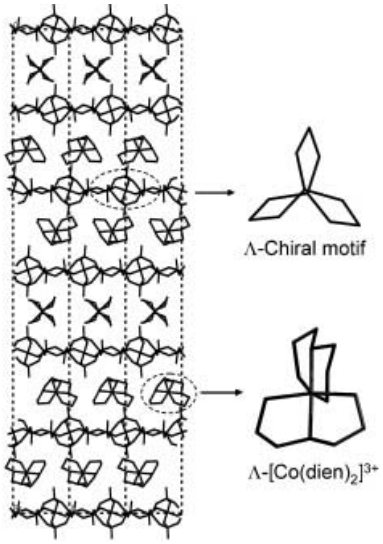

Figure 5. The [3.3.3]propellane-like chiral motif and the chiral $[Co(dien)_2]^{3+}$ ions occluded in the interlayer region in **3**.

by a series of [3.3.3]propellane-like chiral motifs exclusively with the Λ configuration. Both the complex cation and the chiral structural motif have the same C_2 symmetry. If the metal complexes with the "wrong" configuration are inserted into the experimental lattice, no hydrogen bonds will be formed between the complex template and the inorganic host. The difference in hydrogen bond energy of the host–guest between the experimental and the reversed hypothetical frameworks is $-44.85\ kJ\,mol^{-1}$ per complex. This explains why a structural motif with the Λ configuration is induced instead of the Δ configuration in the lattice.

In a chiral layered aluminophosphate $[Co(tn)_3][Al_3P_4O_{16}]\cdot 2H_2O$ (**4**) with a 4.6.8-net, one enantiomer of the metal complex with C_1 symmetry and the Δ configuration is present (Figure 6),[23] therefore, the chiral capped six-membered-ring motif has C_1 symmetry and exclusively exhibits the Δ configuration (Figure 6). The above discussion helps to demonstrate the correspondence of the symmetry and configuration of the chiral, inorganic structural motif to that of the complex cation in chiral frameworks. In our recently reported two cobalt-complex-templated zinc phosphates, $[Co^{II}(en)_3]_2[Zn_6P_8O_{32}H_8]$ (**5**) and $[Co^{III}(en)_3][Zn_8P_6O_{24}Cl]\cdot 2H_2O$ (**6**),[28] a pair of enantiomers with chiral, inorganic structural motifs are induced by a pair of enantiomers with chiral complex cations. Figure 7 shows a pair of enantiomers with chiral complexes induced by a pair of enantiomers with [3.3.3]propellane-like chiral structural motifs in the layered structure of **5**. The complex cations have C_2 and C_1 symmetry, and the structural motif has C_1 symmetry. Figure 8 shows a

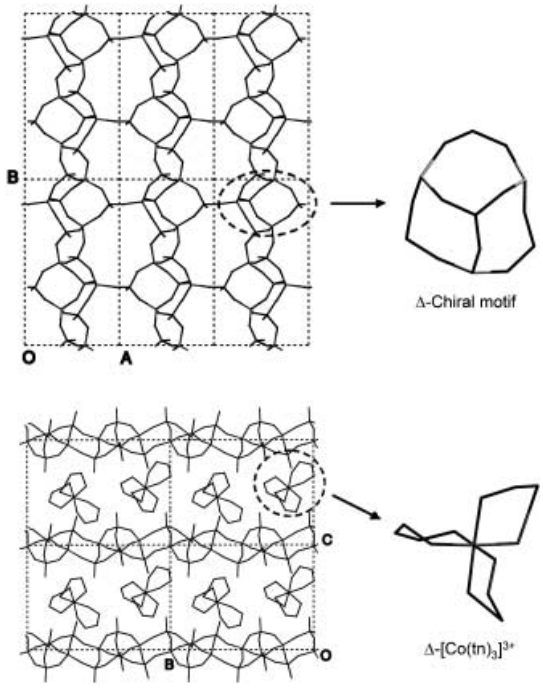

Figure 6. The 4.6.8-net sheet in **4**. The capped six-membered-ring chiral motif and the chiral metal complex occluded in the interlayer region are shown.

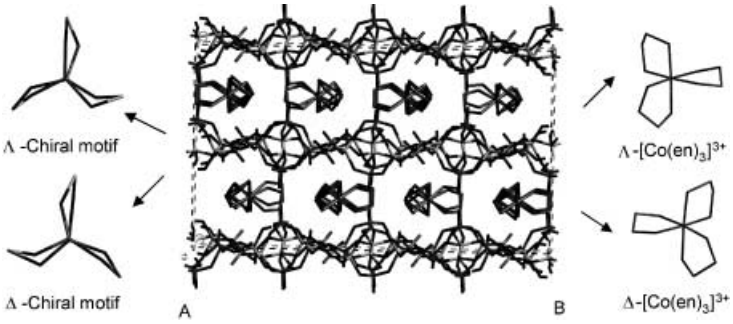

Figure 7. A pair of enantiomers of [3.3.3]propellane-like chiral structural motifs in the inorganic layer, and a pair of enantiomers of chiral complexes alternatively residing the interlayer region in **5.**

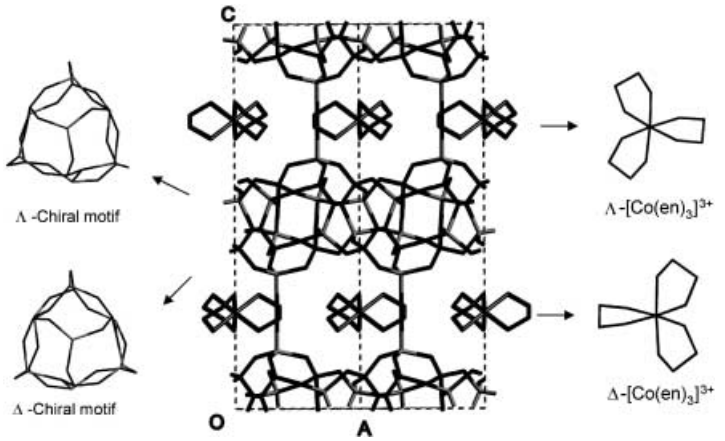

Figure 8. A pair of enantiomers of caplike chiral structural motifs in the inorganic framework and a pair of enantiomers of chiral complexes alternatively residing in different channels in **6.**

pair of enantiomers with chiral complexes induced by a pair of enantiomers with caplike chiral structural motifs in the 3D open framework structure of **6.** The chiral structural motif is composed of six four-membered and three three-membered rings. The chiral complex cation in **6** has D_3 symmetry, and the chiral structural motif has C_3 symmetry. Notice that the chiral $[Co(en)_3]^{3+}$ or $[Co(en)_3]^{2+}$ templates in a regular octahedron have D_3 symmetry. The above two examples suggest that the template can impose its individual symmetry constraint onto the inorganic structural motif. That is, the chiral structural motif has a subgroup of the point-group symmetry of the complex. Notably, in these two structures the metal complex with the Δ configuration forms hydrogen bonds to the structural motifs with both the Δ and Λ configuration, or vice versa. However, in both cases, if the configuration of each metal complex is replaced by the "wrong" enantiomer, the number of hydrogen bonds will be reduced and the hydrogen bond energy of the host – guest will become unfavorable. This indicates that hydrogen bonds play an important role in determining the stereospecificity between the metal-complex templates and the inorganic structural motifs.

More interestingly, it is found that the [3.3.3]propellane-like chiral structural motif is frequently associated with the chiral metal-complex template as in compounds **2**, **3**, and **5**. Recently, two new gallium phosphates $[Co(en)_3][Ga_3P_4O_{16}]\cdot 3H_2O$ and *trans*-$[Co(dien)_2][Ga_3P_4O_{16}]\cdot 3H_2O$, whose structures are isostructural to the layered aluminophosphates $[Co(en)_3][Al_3P_4O_{16}]\cdot 3H_2O$[16] and *trans*-$Co(dien)_2\cdot Al_3P_4O_{16}\cdot 3H_2O$,[22] have been synthesized by us. Both of the structures feature a chiral structural motif. Structurally, it appears that the symmetry and configuration of the [3.3.3]propellane-like structural motif is a good match with that of the metal-complex template. Further understanding of the formation mechanism for the chiral structural motif around the chiral metal complex would facilitate the design of new chiral inorganic microporous materials.

Conclusion

In this work, we have studied the role of a chiral-complex template to determine the stereospecificity of an inorganic framework structure. Upon investigating the structures of a new open-framework zinc phosphate $[Co^{II}(en)_3][Zn_4(H_2PO_4)_3(HPO_4)_2(PO_4)(H_2O)_2]$ and several chiral-complex-templated metal phosphates, we reach the following conclusions: 1) An asymmetric microenvironment can be invariably induced in the inorganic framework as a result of chirality transfer from chiral metal complexes. 2) There exists molecular recognition between the host framework and the guest chiral template; this allows the symmetry and configuration information of the guest template to be passed onto the inorganic structural motif. 3) The remarkable stereospecific correspondence between the complex template and the inorganic host is attributed to the hydrogen bonding between the host framework and the guest molecules. This work provides some insight into the interactions between a chiral template and a corresponding inorganic framework. It is believed that the approach, which employs a rigid chiral template to impart its chirality to the inorganic open-framework, will eventually be successful.

Acknowledgement

This work is supported by the National Natural Science Foundation of China and the State Basic Research Project of China (G2000077507).

[1] M. M. J. Treacy, J. M. Newsam, *Nature* **1988**, *332*, 249 – 251.
[2] a) T. E. Mallouk, J. A. Gavin, *Acc. Chem. Res.* **1998**, *31*, 209 – 217; b) G. Cao, M. E. Garcia, M. Alcalá, L. F. Burgess, T. E. Mallouk, *J. Am. Chem. Soc.* **1992**, *114*, 7574 – 7575.
[3] A. Corma, M. Iglesias, C. del. Pino, F. Sánchez, *J. Chem. Soc. Chem. Commun.* **1991**, 1253 – 1254.
[4] a) A. Joy, S. Uppili, M. R. Netherton, J. R. Scheffer, V. Ramamurthy, *J. Am. Chem. Soc.* **2000**, *122*, 728 – 729; b) K. Chong, J. Sivaguru, T. Shichi, Y. Yoshimi, V. Ramamurthy, J. R. Scheffer, *J. Am. Chem. Soc.* **2002**, *124*, 2858 – 2859.
[5] R.-G. Xiong, X-Z. You, B. F. Abrahams, Z. Xue, C.-M. Che, *Angew. Chem.* **2001**, *113*, 4554—4557; *Angew. Chem. Int. Ed*. **2001**, *40*, 4422 – 4425.
[6] M. E. Davis, *Acc. Chem. Res.* **1993**, *26*, 111 – 115.
[7] M. E. Davis, R. F. Lobo, *Chem. Mater.* **1992**, *4*, 756 – 768.
[8] M. W. Anderson, O. Terasaki, T. Ohsuna, A. Philippou, S. P. MacKay, A. Ferreira, J. Rocha, S. Lidin, *Nature* **1994**, *367*, 347 – 351.
[9] W. T. A. Harrison, T. E. Gier, G. D. Stucky, R. W. Broach, R. A. Bedard, *Chem. Mater.* **1996**, *8*, 145 – 151.
[10] S. Neeraj, S. Natarajan, C. N. R. Rao, *Chem. Commun.* **1999**, 165 – 166.
[11] S. Ayyappan, X. Bu, A. K. Cheetham, C. N. R. Rao, *Chem. Mater.* **1998**, *10*, 3308 – 3310.
[12] V. Sghomonian, Q. Chen, R. C. Haushalter, J. Zubieta, C. J. O'Connor, *Science* **1993**, *259*, 1596 – 1599.
[13] R. J. Francis, S. O'Brien, A. M. Fogg, P. S. Halasyamani, D. T. Loiseau, G. Férey, *J. Am. Chem. Soc.* **1999**, *121*, 1002 – 1015.
[14] T. E. Gier, X. Bu, P. Feng, G. D. Stucky, *Nature* **1998**, *395*, 154 – 157.
[15] Y. Guo, Z. Shi, J. Yu, J. Wang, Y. Liu, N. Bai, W. Pang, *Chem. Mater.* **2001**, *13*, 203 – 207.
[16] K. Morgan, G. Gainsford, N. Milestone, *J. Chem. Soc. Chem. Commun.* **1995**, 425 – 426.
[17] a) G. A. Jeffrey, *An Introduction to Hydrogen Bonding*, 1st ed., Oxford University Press, New York, **1997**; b) J. Isrealachvili, *Intermolecular & Surface Forces*, 2nd ed., Academic Press, London, **1992**; c) N. B. Bowden, M. Weck, S. I. Choi, G. M. Whitesides, *Acc. Chem. Res.* **2001**, *78*, 617 – 622.
[18] A. K. Cheetham, G. Férey, T. Loiseau, *Angew. Chem.* **1999**, *112*, 3466-3492; *Angew. Chem. Int. Ed.* **1999**, *38*, 3268 – 3292 and references therein.
[19] C. N. R. Rao, S. Natarajan, A. Choudhury, S. Neeraj, A. A. Ayi, *Acc. Chem. Res.* **2001**, *34*, 80 – 87, and references therein.
[20] J. Yu, R. Xu, *Acc. Chem. Res.* **2003**, *36*, 481 – 490.
[21] M. J. Gray, J. D. Jasper, A. P. Wilkinson, *Chem. Mater.* **1997**, *9*, 976 – 980.
[22] D. A. Bruce, A. P. Wilkinson, M. G. White, J. A. Bertrand, *J. Solid State Chem.* **1996**, *125*, 228 – 233.
[23] D. A. Bruce, A. P. Wilkinson, M. G. White, J. A. Bertrand, *J. Chem. Soc. Chem. Commun.* **1995**, 2059 – 2060.
[24] D. J. Williams, J. S. Kruger, A. F. McLeroy, A. P. Wilkinson, J. C. Hanson, *Chem. Mater.* **1999**, *11*, 2241 – 2249.
[25] S. M. Stalder, A. P. Wilkinson, *Chem. Mater.* **1997**, *9*, 2168 – 2173.
[26] Y. Wang, J. Yu, Y. Li, Z. Shi, R. Xu, *J. Solid State Chem.* **2003**, *170*, 176 – 181.
[27] G. Yang, S. C. Sevov, *Inorg. Chem.* **2001**, *40*, 2214 – 2215.
[28] J. Yu, Y. Wang, Z. Shi, R. Xu, *Chem. Mater.* **2001**, *13*, 2972 – 2978.
[29] Y. Wang, J. Yu, M. Guo, R. Xu, *Angew. Chem.* **2003**, *115*, 4223 – 4226; *Angew. Chem. Int. Ed.* **2003**, *34*, 4089 – 4092.
[30] SMART and SAINT software package; Siemens Analytical X-ray Instruments, Madison, WI, **1996**.

[31] G. M. Sheldrick, SHELXL Program, version 5.1, Siemens Industrial Automation, Madison, WI, **1997**.
[32] E. de Vos Burchart, *Studies on Zeolites; Molecular Mechanics*, *Framework Stability and Crystal Growth*, Ph.D. Thesis, Technische Universiteit Delft, **1992**.
[33] S. L. Mayo, B. D. Olafson, W. A. Goddard, *J. Phys. Chem.* **1990**, *94*, 8897–8909.
[34] A. J. Ramirez-Cuesta, C. H. Mitchell, P. M. Roger, *J. Chem. Soc. Faraday Trans.* **1998**, *94*, 2249–2255.
[35] Cerius^2@Molecular simulations/Biosym Corporation, **1995**.
[36] F. A. Cotton, G. Wilkinson, *Advanced Inorganic Chemistry*, 5th Ed., **1988**, Wiley, New York, p. 93.

Received: April 12, 2003 [F5040]

